

# (Cd,Mg)Te Crystals for Picosecond-Response Optical-to-X-Ray Radiation Detectors

J. Cheng,<sup>1,2</sup> G. Chen,<sup>1,2</sup> D. Chakraborty,<sup>1,2</sup> S. Kutcher,<sup>3</sup> J. Wen,<sup>3</sup> H. Chen,<sup>3</sup> S. Trivedi,<sup>3</sup> and Roman Sobolewski,<sup>1,2,4</sup>

<sup>1</sup>Materials Science Graduate Program, University of Rochester

<sup>2</sup>Laboratory for Laser Energetics, University of Rochester

<sup>3</sup>Brimrose Technology

<sup>4</sup>Departments of Electrical and Computer Engineering and Physics and Astronomy, University of Rochester

We demonstrate a photodetector sensitive to both optical and x-ray picosecond pulses based on our in-house grown cadmium magnesium telluride (Cd,Mg)Te single crystal. Specifically, we developed In-doped Cd<sub>0.96</sub>Mg<sub>0.04</sub>Te material and discuss its femtosecond optical photoresponse, as well as the detector performance, like <100-pA dark current and up to 0.22-mA/W responsivity for 780-nm-wavelength optical radiation. The detector exposed to Ti fluorescence (K $\alpha$ ) x-ray pulses at 4.5 keV, generated by a free-electron laser beam with a central energy of 9.8 keV and <100-fs pulse width, exhibited readout-electronics-limited 200-ps full-width-at-half-maximum photoresponse, demonstrating that it is suitable for coarse timing in free-electron laser x-ray/optical femtosecond pump-probe spectroscopy applications.

Ultrafast, solid-state detectors covering the optical/near-infrared to x-ray radiation spectrum are in high demand due to their versatile applications, including optical/x-ray subpicosecond pump-probe spectroscopy. Only a few available photodetectors can adequately do this job. Si-based photodetectors cover a wide range of wavelengths and can operate in the x-ray range; however, they degrade due to environmental effects as well as radiation damage.<sup>1</sup> Photodetectors based on metal-semiconductor-metal (MSM) structures with interdigitated electrodes, fabricated on low-temperature-grown GaAs (LT-GaAs), such as, e.g., a HAMAMATSU G4176-03 photodetector, are typically designed for picosecond temporal response for optical signals.<sup>2</sup>

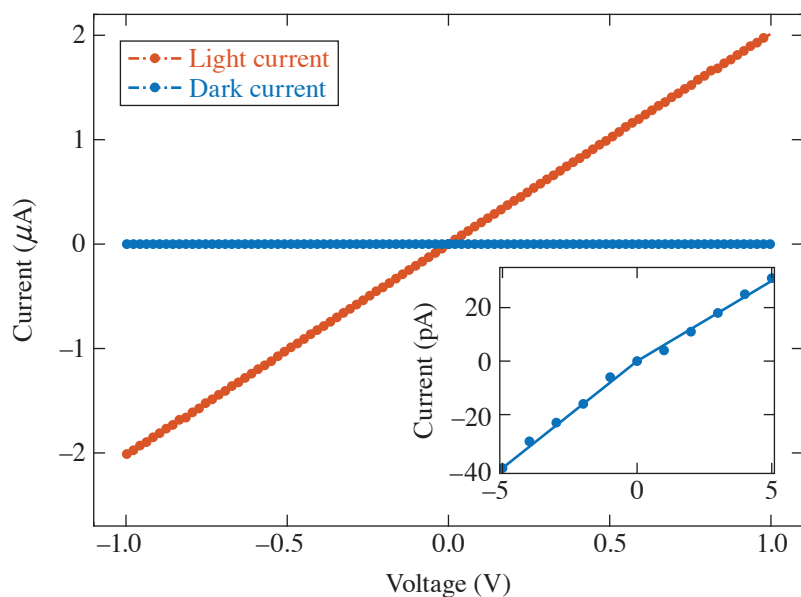
We demonstrate that (Cd,Mg)Te (CMT) is a very promising candidate as a dual-optical/x-ray ultrafast detector. CMT is a ternary compound with a tunable direct energy gap from ~1.5 eV to 3.1 eV by changing the Mg content.<sup>3</sup> At the same time, due to the presence of a high-stopping-power Te element, crystals very effectively absorb high-energy x-ray photons [for a 1-mm-thick (Cd,Mn)Te crystal, the 1/e absorption drop occurs at 94.2 keV; Ref. 4]. The carrier lifetime of doped CMT can be comparable to that of LT-GaAs, which is critical in ultrafast temporal resolution. Ultralow device leakage current is another essential criterion, and CMT can have a lower leakage current than GaAs in the same MSM arrangement because of its larger band gap.

The Cd<sub>1-x</sub>Mg<sub>x</sub>Te ( $x$  is between 0 to 0.45) crystal exhibits the zinc blende structure and it is the latest member of ternary alloys that include (Cd,Zn)Te and (Cd,Mn)Te, both well known for x-ray detection applications.<sup>4,5</sup> (Cd,Mg)Te possesses all the necessary qualities for an optimal radiation detector, like high material density (5.83 g/cm<sup>3</sup>), high effective mass (49.5), ultrahigh resistivity (~10<sup>10</sup>  $\Omega$ cm), and good electron mobility lifetime ( $\mu\tau$ ) product (>10<sup>-4</sup> cm<sup>2</sup>V<sup>-1</sup>) (Ref. 6). In addition, the CMT “parent” crystals, CdTe and MgTe, exhibit very close lattice constants, 6.48 Å and 6.42 Å, respectively,<sup>7</sup> leading to a high-quality growth of CMT single crystals. At room temperature, the band gap of Cd<sub>1-x</sub>Mg<sub>x</sub>Te is a linear function of  $x$ , increasing at a rate of around 15 meV per Mg atomic percent.<sup>3</sup> At  $x = 0$ , the CdTe band gap is 1.503 eV (Ref. 3).

Brimrose developed an innovative in-house procedure to purify magnesium to the highest achievable level. This proprietary technique involves sublimation under dynamic vacuum. The process uses two ampoules—the inner pyrolytic boron nitride (PBN)

ampoule is placed inside the graphitized fused-silica ampoule of a length a little longer than the PBN ampoule. Thus Mg (in molten or vapor phase) is prevented from reacting with the outer fused-silica ampoule, which is connected to the high-vacuum system.

The vertical Bridgman method was used to grow high-purity CMT single crystals.<sup>8</sup> Approximately 1-in.-diam ingots are grown, sliced into 1-mm-thick wafers (Fig. 1), and, finally, cut into suitably sized samples (from  $4 \times 4 \text{ mm}^2$  to  $10 \times 10 \text{ mm}^2$ ). During the growth process, the content of Mg can be modified and selective dopants can be added. Additionally, post-growth annealing can be optimized in order to engineer a material that will exhibit characteristics required for a given application. We determined that 3% to 8% Mg and 2% to 5% In doping led to CMT crystals with a suitable band gap and acceptable electron mobility times lifetime ( $\mu\tau$ ) product ( $>10^{-4} \text{ cm}^2\text{V}^{-1}$ ), as well as a large enough resistivity ( $>10^{10} \text{ W-cm}$ ) for detector applications.<sup>9</sup>



E30447JR

Figure 1

Current–voltage ( $I$ – $V$ ) characteristics under light (orange) and dark (blue) conditions for a tested CMT device. The inset shows the dark current  $I$ – $V$  in detail (bulk measurement across a CMT sample).

We selected the Mg concentration in  $(\text{Cd},\text{Mg})\text{Te}$  the way that the crystal should have the band gap compatible for an optical photodetector operation within the tunability of a Ti:sapphire femtosecond pulsed laser. For this purpose, we performed optical reflection and transmission spectra measurements using a PerkinElmer Lambda 900 spectrometer with samples placed at normal incidence. The Tauc plot for direct-band-gap material<sup>10</sup> combines the collected experimental spectra and presents the crystal absorption spectrum. We observed a sharp optical transition edge and the band gap  $E_G = 1.57 \text{ eV}$ , with a small absorption tail below  $E_G$  that is typically related to shallow sub-gap trap states. For photons with energies above  $E_G$  we see the full absorption. In-doped,  $\text{Cd}_{0.96}\text{Mg}_{0.04}\text{Te}$  crystals were used in the subsequent detector fabrication.

Photoresponse measurements were carried out in the surface-mode configuration with an optical beam, generated by a Ti:sapphire laser (780-nm wavelength) focused between the electrodes. A bank of neutral-density filters was used to control the laser intensity and the current–voltage ( $I$ – $V$ ) characteristics were collected using a digital sourcemeter. Figure 1 demonstrates a strong photoconductive effect of our CMT MSM diode. Under optical excitation (orange curve; 20-mW laser power) a photocurrent reaches  $\sim 2 \mu\text{A}$  at a 1-V bias. The  $I$ – $V$  dependence is linear, indicating an absence of Schottky barriers. At the same time, the dark current (blue curve) is completely negligible. In the measurements above, we used the bias voltage only up to 1 V in order to avoid a possible breakdown between the electrodes separated by just  $25 \mu\text{m}$ .

Further systematic photoresponse characterization was carried out on our CMT diodes, including the photocurrent and responsivity dependencies on voltage for a wide range of incident optical powers. Figure 2 shows a family of the responsivity traces as a function of detector bias voltage for incident power in the 20- $\mu\text{W}$  to 20-mW range. We note that for our device, the responsivity increases as the decrease of incident power. This phenomenon is related to the intrinsic gain mechanism in semiconductors characterized by a substantial disparity in electron and hole mobilities. The greatest responsivity obtained is 0.22 mA/W, but we

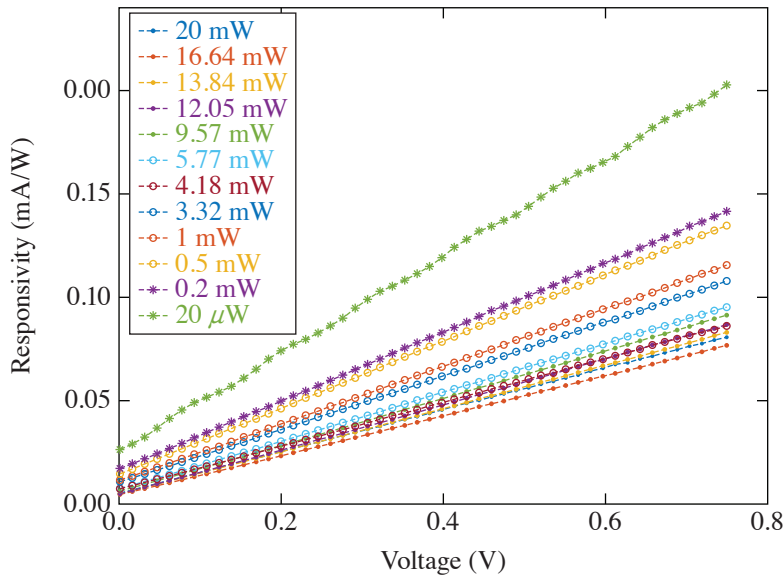


Figure 2  
CMT diode responsivity versus bias voltage for several incident power levels of the 780-nm-wavelength radiation (bulk measurement across a CMT sample).

E30448JR

expect to increase it very substantially when the surface detector structure is fabricated in a form of a large-area interdigitated-electrode configuration to increase the collection of carriers generated by the light/x-ray radiation.

The CMT diode was also a subject of preliminary tests at the SLAC National Accelerator Laboratory. Figure 3 presents an actual oscilloscope image of the diode response to an x-ray pulse. To prevent damage to the detector, a <100-fs-wide, 9.8-keV central energy, and 120-Hz repetition rate train of x-ray pulses from a free-electron laser were directed onto a titanium target, so the signal shown in Fig. 3 is actually the x-ray fluorescence at the Ti  $K_{\alpha}$  edge (4.5 keV). The observed signal has an  $\sim 0.2$ -ns FWHM and a <100-ps rise time, limited by the detection electronics. The above parameters make our device suitable for course timing of optical/x-ray subpicosecond pump-probe spectroscopy experiments.

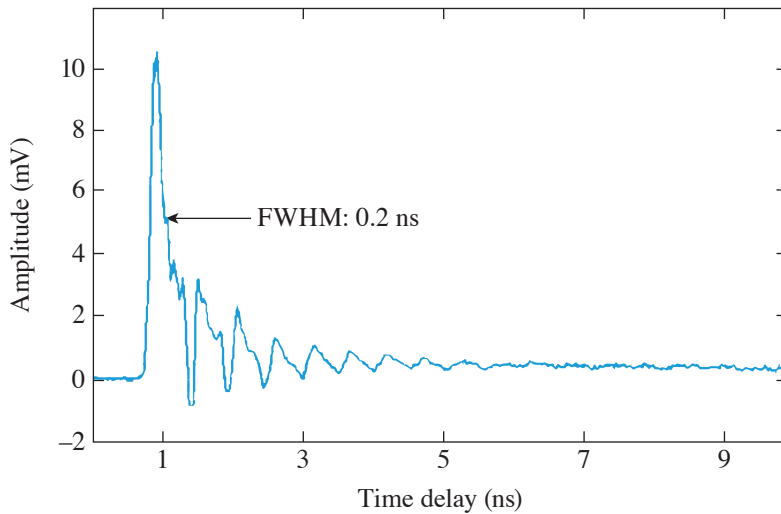


Figure 3  
Oscilloscope plot of the time-resolved CMT detector response to a pulsed x-ray signal generated at the SLAC National Accelerator Laboratory. After-pulse oscillations are due to the impedance mismatch in the electronics detection channel.

E30449JR

We demonstrate that (Cd,Mg)Te is a very promising candidate for ultrafast optical/near-infrared to x-ray radiation detector applications. We selected the In-doped  $\text{Cd}_{0.96}\text{Mg}_{0.04}\text{Te}$  crystal for our detectors, so its optical bandwidth made it sensitive to the Ti:sapphire light, while In doping resulted in an ultrahighly resistive material characterized by a <100-pA leakage dark current and 2.4-ps electron relaxation time. The detector was tested at the SLAC National Accelerator Laboratory and exhibited a

response signal of 200-ps FWHM (electronics limited) when exposed to Ti fluorescence ( $K_{\alpha}$ ) x-ray pulses at 4.5 keV, generated by a free-electron laser beam with the central energy of 9.8 keV and <100-fs pulse width. The latter confirms CMT suitability for the free-electron laser pump–probe spectroscopy timing applications.

The authors thank Drs. Takahiro Sato and David Fritz from the SLAC National Accelerator Laboratory for providing Fig. 3. This work was supported in part by the Department of Energy Phase I SBIR program under Award: DE-SC0021468 and monitored by Dr. Eliane S. Lessner and Dr. Yiping Feng (DOE/SLAC).

1. M. Shanmugam *et al.*, *J. Instrum.* **10** (2015).
2. Hamamatsu Preliminary Data, Ultrafast Response of Several Tens Picosecond; G4176-03, Accessed 27 February 2023, [https://www.datasheet.cloud/pdfviewer?url=https%3A%2F%2Fpdf.datasheet.cloud%2Fdatasheets-1%2Fhamamatsu\\_photonics\\_k.k.%2FG4176-03.pdf](https://www.datasheet.cloud/pdfviewer?url=https%3A%2F%2Fpdf.datasheet.cloud%2Fdatasheets-1%2Fhamamatsu_photonics_k.k.%2FG4176-03.pdf).
3. E. G. LeBlanc *et al.*, *J. Electron. Mater.* **46**, 5379 (2017).
4. A. S. Cross *et al.*, *Nucl. Instrum. Methods Phys. Res. A* **624**, 649 (2010).
5. Y. Eisen, A. Shor, and I. Mardor, *IEEE Trans. Nucl. Sci.* **51**, 1191 (2004).
6. S. B. Trivedi *et al.*, *Next Generation Semiconductor-Based Radiation Detectors Using Cadmium Magnesium Telluride (Phase I Grant—DE-SC0011328)*, U.S. Department of Energy, Washington, DC, Report DOE/11172015-Final (2017).
7. J.-H. Yang *et al.*, *Phys. Rev. B* **79**, 245202 (2009).
8. S. B. Trivedi *et al.*, *J. Cryst. Growth* **310**, 1099 (2008).
9. J. Serafini *et al.*, *Semicond. Sci. Technol.* **34**, 035021 (2019).
10. J. Tauc, R. Grigorovici, and A. Vancu, *Phys. Stat. Sol. (B)* **15**, 627 (1966).